Modern Journal of Health and Applied Sciences *(MJHAS)*

E-ISSN 3078-2791; P-ISSN 3078-2783

Journal homepage: https://mucjournals.muc.edu.ps

Improving Grayscale Medical Images (X-Rays, MRI, CT Scans)

Alaa Hasan Saad Alarajey [1*], and *Kawther H. Al-khafaji* [1]

[1] Kufa University Faculty of Education for Women.

ARTICLE INFO

Received: 26th April 2025
Received in revised form: 04th June 2025
Accepted: 08th June 2025
Published: 15th September 2025

***Corresponding Author:**
Alaa Hasan Saad Alarajey
E-mail:
Alah43602@gmail.com

Citation: Hasan Saad Alarajey, A., H. Al-Khafaji, K. Improving Grayscale Medical Images (X-Rays, MRI, CT Scans). *Modern Journal of Health and Applied Sciences*, 2(2), 73-85

DOI: https://doi.org/10.70411/MJHAS.2.2.2025238

ABSTRACT

Medical images provide critical information that physicians need to diagnose a condition and make appropriate treatment decisions. The diagnostic process relies heavily on human perception. Unfortunately, the potential for perceptual errors is unacceptable, impacting patients' lives. Therefore, image enhancement represents a crucial step in supporting medical diagnosis by improving its quality. In this research, we applied a new algorithm to enhance X-ray, MRI, and CT images. This algorithm aims to improve contrast and sharpness based on an empirical equation using trigonometric functions (cos) based on Fourier transforms and changing the value of one of its main parameters. Nasal polyps were more clearly identified in X-rays, and brain tumours were more clearly identified in MRI and CT scans. Histograms were used before and after enhancement, and we observed a significant difference between the original and enhanced images in terms of the histogram shift toward unity, demonstrating the success of this algorithm in improving contrast and organ prominence.

Keywords: X-rays, MRI, CT scans, Medical images, Improve medical images, Medical image Enhancement.

1. Introduction

Image enhancement is a fundamental stage of image processing. This enhancement is often used to improve image quality by highlighting specific information and removing unnecessary details based on user requirements. Image enhancement has two functions: increasing visual impact and facilitating computer processing. Image enhancement offers numerous advantages, including noise reduction, edge sharpening, brightness enhancement, and contrast enhancement (Al-Khafaji & Sahib, 2024; Hussain et al., 2022). Medical images are often produced with low contrast, low intensity, noise, and distortion due to limitations in medical equipment. Due to their low quality, these images cannot be used for diagnosis. Therefore, to create high-quality images with more information that facilitate better analysis, careful image processing is necessary (Pourasad & Cavallaro, 2021). Medical imaging is a rapidly expanding area of study that is used to identify and treat diseases early. Image processing is becoming increasingly important in the healthcare sector. Medical imaging is a group of technologies that visualise the human body to diagnose, track, or treat medical disorders. It includes technologies such as endoscopy, computed tomography (CT), positron emission tomography (PET), magnetic resonance imaging (MRI), ultrasound, X-rays, and others. To assist physicians worldwide in diagnosis, treatment, and prevention, medical imaging is essential (Agrawal et al., 2025; Li et al., 2019; Pinto-Coelho, 2023). In this paper, a novel algorithm based on empirical equations and trigonometric functions is proposed for medical image enhancement, and it is applied to X-ray, MRI, and CT images.

2. Medical Images

Many medical imaging techniques have been employed to examine anatomical features, including muscles, bones, blood vessels, tissue types, and diseased areas such as cancer (Kumari, 2025; Rehman & Mir, 2025; Sule & Ampofo, 2025). Therefore, this work focuses primarily on the importance of improving medical images for accurate analysis and diagnosis. This section will cover three medical imaging methods: magnetic resonance imaging (MRI), computed tomography (CT), and X-rays.

2. 1. X-Ray Images

X-rays are used to image the internal structure of the human body and are among the most commonly used diagnostic tools in the medical field. They help radiologists identify internal issues by providing images of the body's internal anatomy. It is the most practical imaging technique for detecting bone fractures. Despite its many benefits, X-ray technology produces images with little contrast. The amount of liquid in the human body is the primary cause of the low contrast of X-ray images. Increasing the X-ray's capacity to take images could damage a person's body or bones (Akbar et al., 2025; Fan et al., 2025; Ou et al., 2021).

2. 2. Magnetic Resonance Images (MRI)

The medical imaging technique known as magnetic resonance imaging (MRI) is founded on the same ideas as spectroscopy using nuclear magnetic resonance. The most effective and noninvasive method for clinical illness diagnosis is magnetic resonance imaging (MRI) (Chen et al., 2023; Reda et al., 2021). The MRI scanner creates images of the body's tissues, organs, and other structures using magnetic and radio waves. It produces images that are superior at portraying fine details. As a result, an MRI scanner may be used to image every tissue in the body. Bones and other tissue with the fewest hydrogen atoms seem dark, but fatty tissue with abundant hydrogen atoms appears considerably brighter. By altering the timing of the radio wave pulses, information regarding the various tissue types that are present can be obtained (Gómez-Guzmán et al., 2023; Nayak et al., 2022).

2. 3. Computed Tomography Images (CT)

CT is a diagnostic technology that combines X-ray equipment with a computer and a cathode ray tube display to produce images of cross sections of the human body. Each profile is reconstructed by the computer into a 2D image of the slice that was scanned. 3D CT can be obtained using spiral CT (Dremel et al., 2025; Falgout et al., 2024; Stewart et al., 2025).

3. Literature Survey

Pourasad and Cavallaro enhanced compressed image quality in 2021 by employing a variety of optimization strategies. They researched various approaches and offered a number of comparison findings. Ultimately, performance measurements were retrieved and examined using cutting-edge techniques. PSNR, MSE, and SSIM were the three performance measures they employed for medical image samples. These measurements perform better than other image processing methods, according to a thorough analysis (Pourasad & Cavallaro, 2021). In 2022, Idowu et al. introduced an enhanced image enhancement method for medical image processing. This method uses three distinct enhancing strategies. The first technique is Unsharp Masking (USM). A Logarithm Transform (LT) receives the output of the USM processing, and the LT output is then fed into an AHE. AMBE, PSNR, Entropy, and Predicted Opinion Score were used to assess the effectiveness of the suggested approach. A reliable result for AMBE and PSNR Entropy was obtained using the suggested approach (Idowu et al., 2022). In 2023, Mouzai et al. suggested an Xray-Net method to improve low-contrast photos using a self-supervised pixel contrast expansion. The approach consists of three primary steps: (1) preprocessing, which includes calculating the average brightness to create an X-ray contrast-based classification; (2) creating a traditional neural network model; and (3) adaptive contrast expansion. When compared to other state-of-the-art techniques, Xray-Net's results show greater performance in low-contrast enhancement (Mouzai et al., 2023). Anitha et al. (2024) improved image quality by removing uniform, Gaussian, and salt-and-pepper noise using various filtering and contrast enhancement approaches (Anitha et al., 2024). In 2024, Babu and Venkatanarayana presented a novel approach to multimodal image fusion for medical imaging (MRI, CT) that utilizes low- and high-frequency weights derived from the CSGWO algorithm. The suggested approach uses quadrupole wavelet transform (QWT) to extract low- and high-frequency components, contrast enhancement in preprocessed images, and cartoon texture (CT)-based analysis. The fusion quality index and other objective criteria were used to assess the suggested approach. The outcomes showed how the suggested approach outperformed alternative approaches and how well it worked to raise the general calibre of medical photographs (Babu & Venkatanarayana, 2024). To regulate the total contrast augmentation, Singh and Raj (2024) suggested a histogram cropping technique based on eight-degree polynomials. Through the use of a single objective fitness function, the technique also establishes an exposure threshold value and a genetic algorithm (GA) to improve the histogram segmentations, guaranteeing constant brightness and reducing information loss. A number of metrics were employed, including the Feature Similarity Index Method (FSIM), Entropy, and PSNR (Yadav & Donvir, 2025). A new AI-powered approach for automatically creating tactile and three-dimensional medical X-ray images was proposed by Yadav and Donvir in 2025. The system generates high-resolution depth maps suitable for tactile display by utilising image processing techniques such as depth estimation and image enhancement. Accuracy and processing time are objective criteria used to assess system performance. This study shows that an automated method to increase access to medical imaging is feasible, which could improve diagnostic precision and advance healthcare inclusivity (Yadav & Donvir, 2025).

4. Mathematical Analysis

We will apply an empirical equation using trigonometric (cosine) transformations because they are the basis for the frequency representation in the Fourier transform, which is used to remove noise and enhance edges on medical images under study (X-rays, MRIs, and CT scans). To improve image quality: -

$$I_E(\mathrm{x,y})=\begin{bmatrix} |\cos(2\pi f I_o(x,y))| \\ |\cos(2\pi f I_o(x,y))| \\ |\cos(2\pi f I_o(x,y))| \end{bmatrix} \ldots\ldots\ldots(1)$$

Where:

$I_E: (x,y)$ is the Enhancing image.

$\mathcal{F}$: is the Frequency coefficient.

$I_O: is\ the\ Original\ image.$

5. Image Acquisition

This work was carried out in MATLAB R2021a. The medical images used for testing are X-rays, MRIs, and CT scans. An X-ray was taken from Sama Clinic in Abu Sakhir District in Najaf Governorate for a patient suffering from nasal polyps. An MRI and CT scan were taken from the German Hospital for the same patient suffering from a brain disease.

6. MATLAB Algorithm Flowchart

Figure 1. illustrates the fundamental algorithm stage:

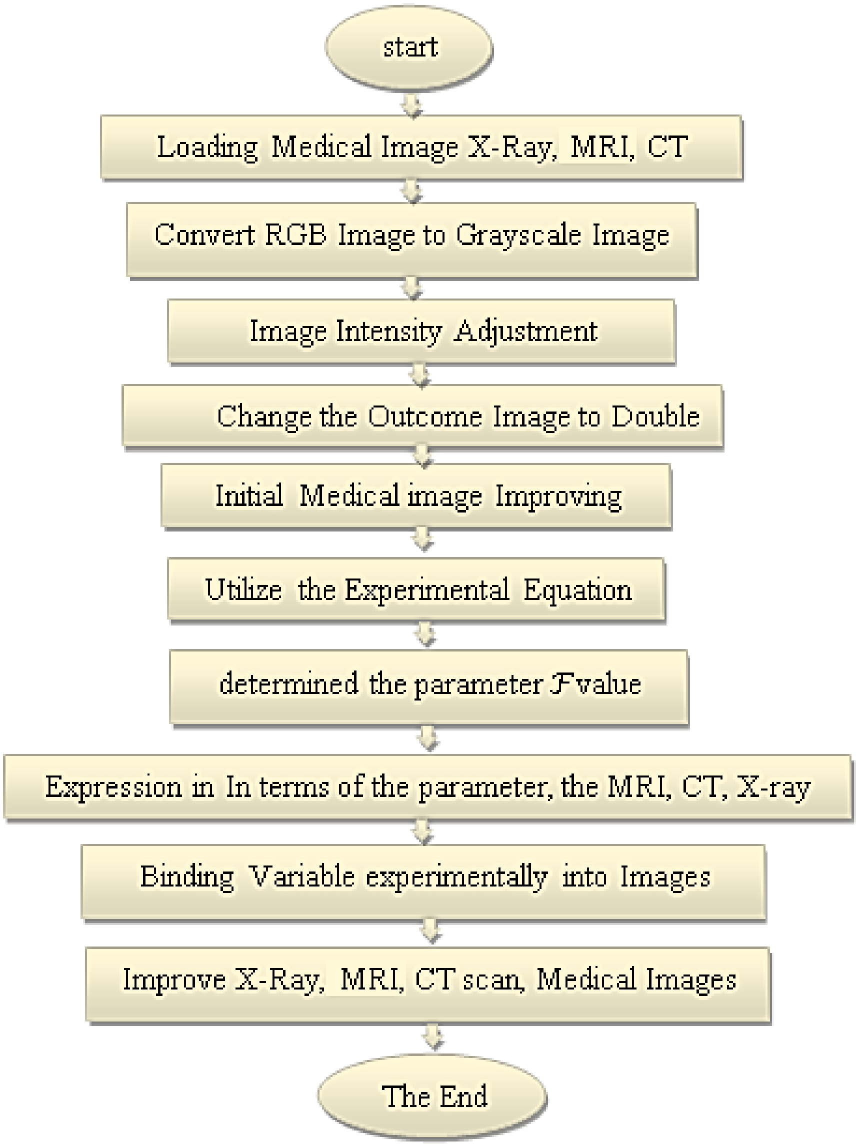

Figure 1. flowchart of propose algorithm

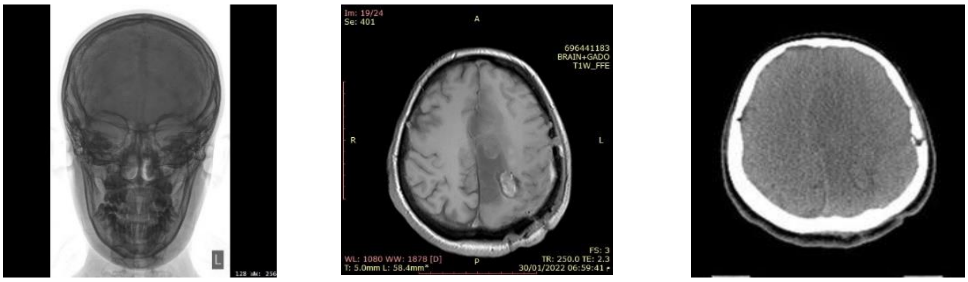

(a) (b) (c)

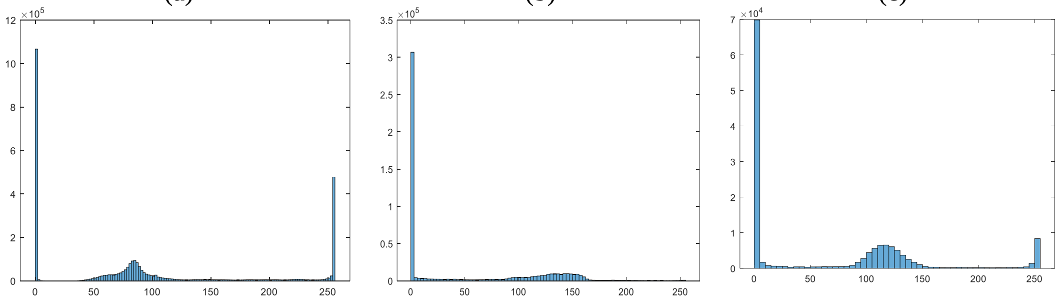

(d) (e) (f)

Figure 2. An original X-ray image, (b) An original MRI image (c) An original CT scan image(d) the related histogram of image in (a),(e) the related histogram of image in (b),(f) the related histogram of image in (c)

7. Method Adopted and Experimental Outcomes

𝓐 𝓑 𝓒

𝓓 𝓔 𝓕


$\mathcal{G}$

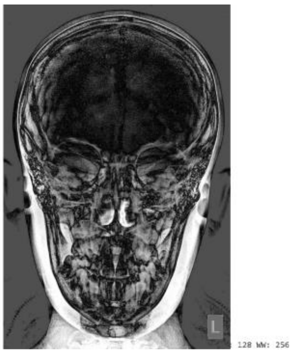
$\mathcal{H}$

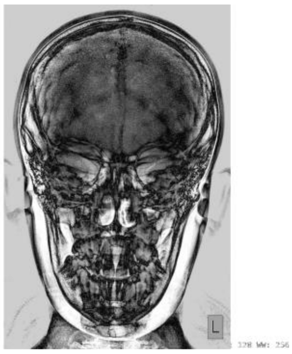
$\mathcal{I}$

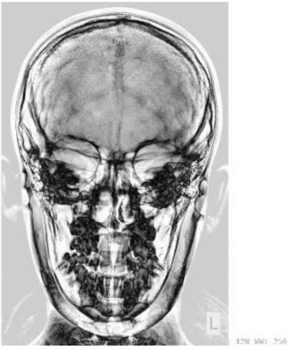
$\mathcal{J}$

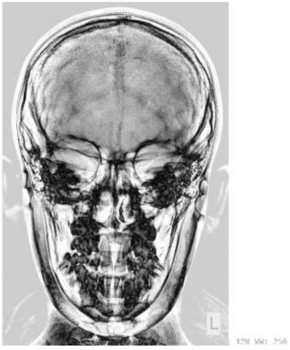
$\mathcal{K}$

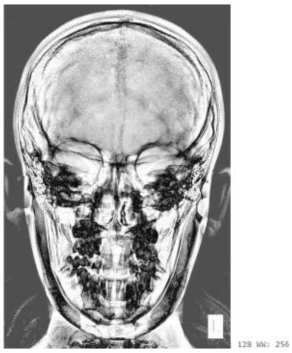
$\mathcal{L}$

Figure 3. The resulting X-ray images ($\mathcal{A}$) resulting image when $\mathcal{F}$ =0.1 ($\mathcal{B}$) resulting image when $\mathcal{F}$ =0.2 ($\mathcal{C}$) resulting image when $\mathcal{F}$ =0.3 ($\mathcal{D}$) resulting image when $\mathcal{F}$ =0.4 ($\mathcal{E}$) resulting image when $\mathcal{F}$ =0.5 ($\mathcal{F}$) resulting image when $\mathcal{F}$ =0.6 ($\mathcal{G}$) resulting image when $\mathcal{F}$ =0.7 ($\mathcal{H}$) resulting image when $\mathcal{F}$ =0.8 ($\mathcal{I}$) resulting image when $\mathcal{F}$ =0.9 ($\mathcal{J}$) resulting image when $\mathcal{F}$ =1.1 ($\mathcal{K}$) resulting image when $\mathcal{F}$ =1.2($\mathcal{L}$) resulting image when $\mathcal{F}$ =0.9

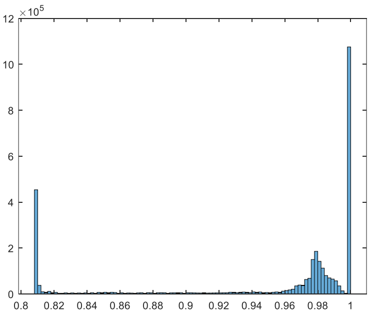
$\mathcal{A}$

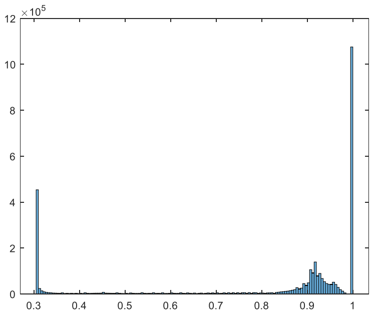
$\mathcal{B}$

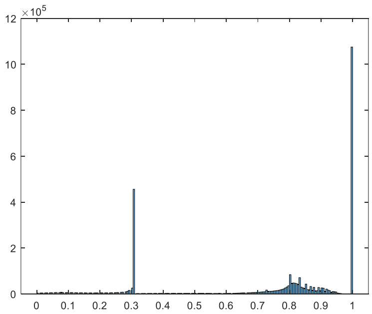
$\mathcal{C}$

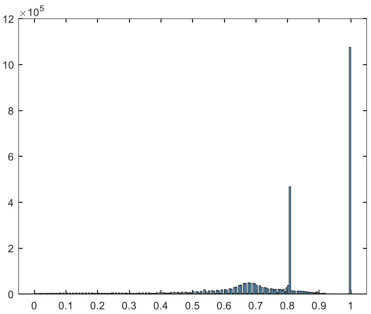
$\mathcal{D}$

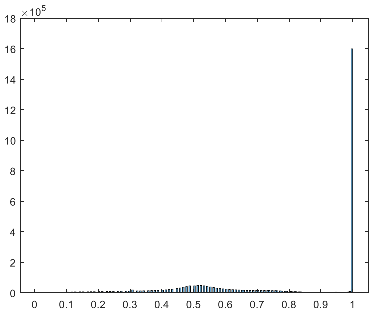
$\mathcal{E}$

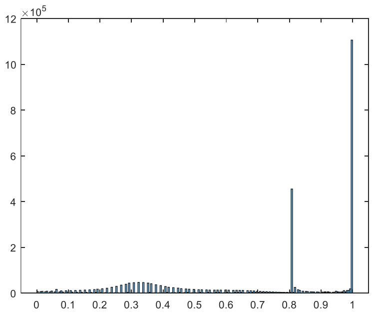
$\mathcal{F}$

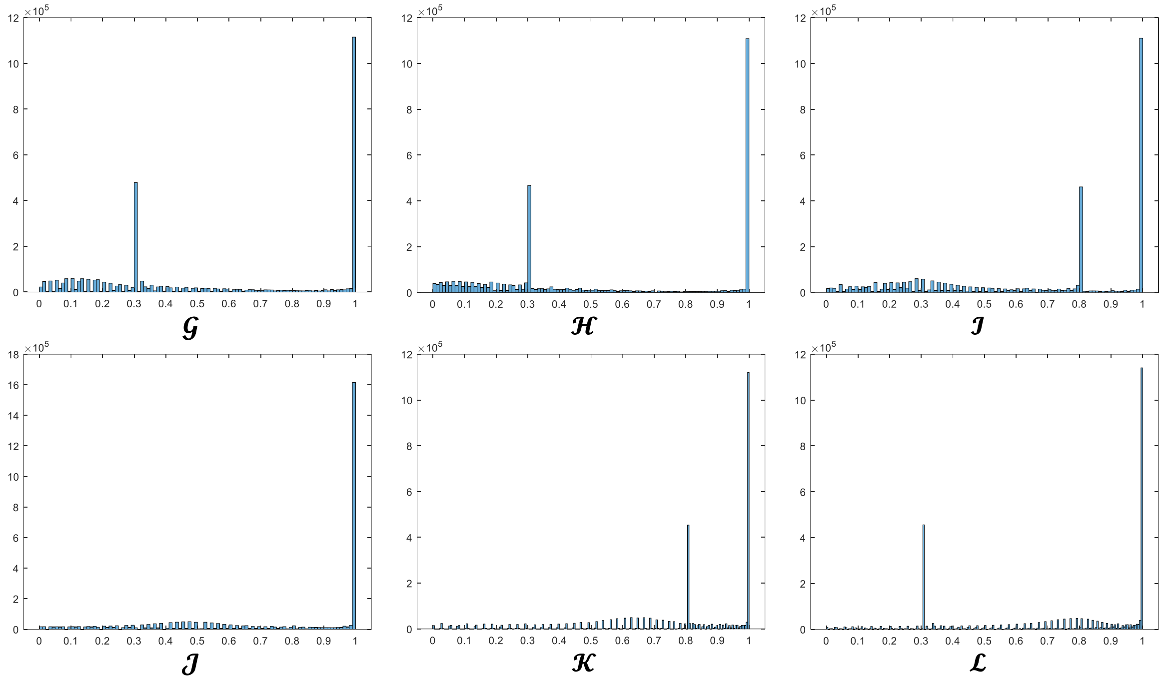

Figure 4. Histogram for X-ray images ($\mathcal{A}$) Histogram for X-ray image when $\mathcal{F}$ =0.1 ($\mathcal{B}$) Histogram for X-ray image when $\mathcal{F}$ =0.2 ($\mathcal{C}$) Histogram for X-ray image when $\mathcal{F}$ =0.3 ($\mathcal{D}$) Histogram for X-ray image when $\mathcal{F}$ =0.4 ($\mathcal{E}$) Histogram for X-ray image when $\mathcal{F}$ =0.5 ($\mathcal{F}$) Histogram for X-ray image when $\mathcal{F}$ =0.6 ($\mathcal{G}$) Histogram for X-ray image when $\mathcal{F}$ =0.7 ($\mathcal{H}$) Histogram for X-ray image when $\mathcal{F}$ =0.8 ($\mathcal{I}$) Histogram for X-ray image when $\mathcal{F}$ =0.9 ($\mathcal{J}$) Histogram for X-ray image when $\mathcal{F}$ =1 ($\mathcal{K}$) Histogram for X-ray image when $\mathcal{F}$ =1.1($\mathcal{L}$) Histogram for X-ray image when $\mathcal{F}$ =1.2

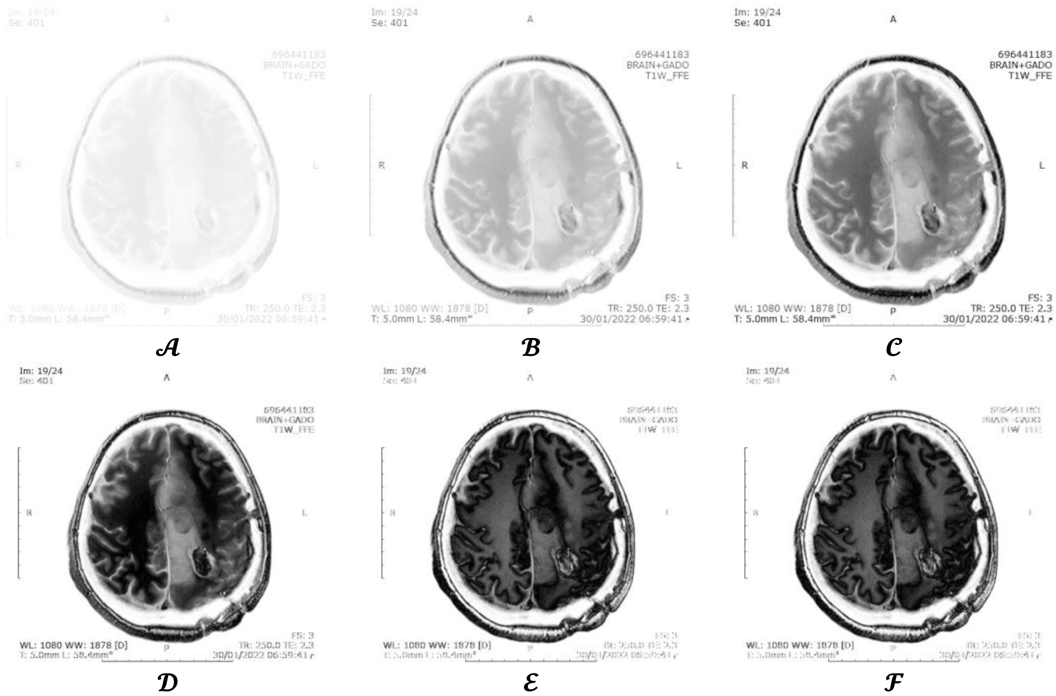

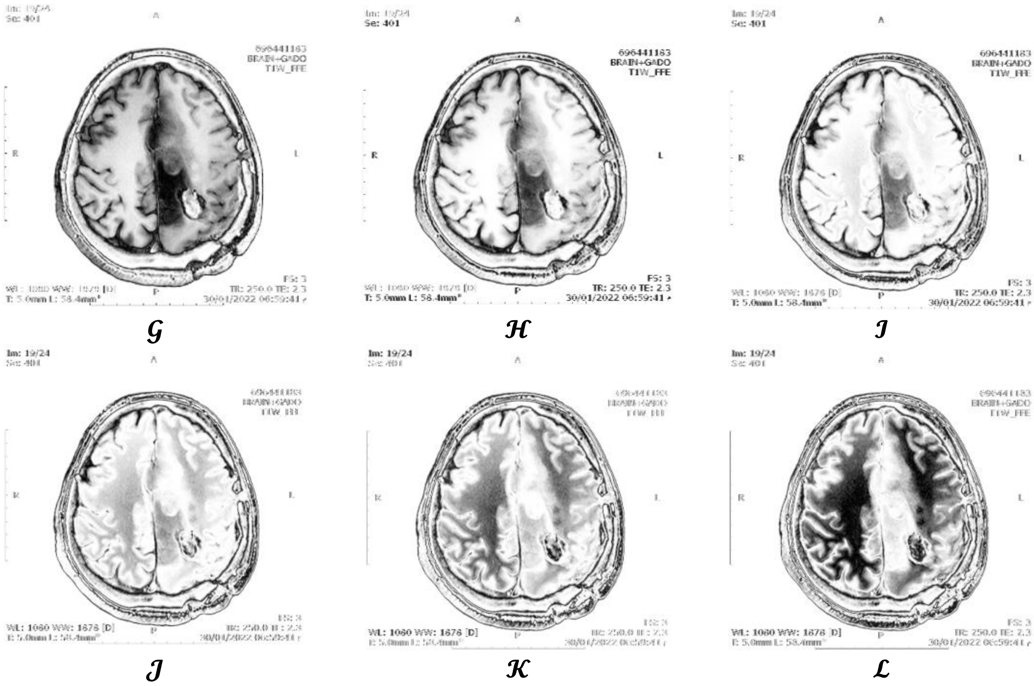

Figure 5. The resulting MRI images $\mathcal{A}$) resulting image when $\mathcal{F}$ =0.1 ($\mathcal{B}$) resulting image when $\mathcal{F}$ =0.2 ($\mathcal{C}$) resulting image when $\mathcal{F}$ =0.3 ($\mathcal{D}$) resulting image when f=0.4 ($\mathcal{E}$) resulting image when $\mathcal{F}$ =0.5 ($\mathcal{F}$) resulting image when $\mathcal{F}$ =0.6 ($\mathcal{G}$) resulting image when $\mathcal{F}$ =0.7 ($\mathcal{H}$) resulting image when $\mathcal{F}$ =0.8 ($\mathcal{I}$) resulting image when f=0.9 ($\mathcal{J}$) resulting image when $\mathcal{F}$ =1.1 ($\mathcal{K}$) resulting image when $\mathcal{F}$ =1.2($\mathcal{L}$) resulting image when $\mathcal{F}$ =0.9

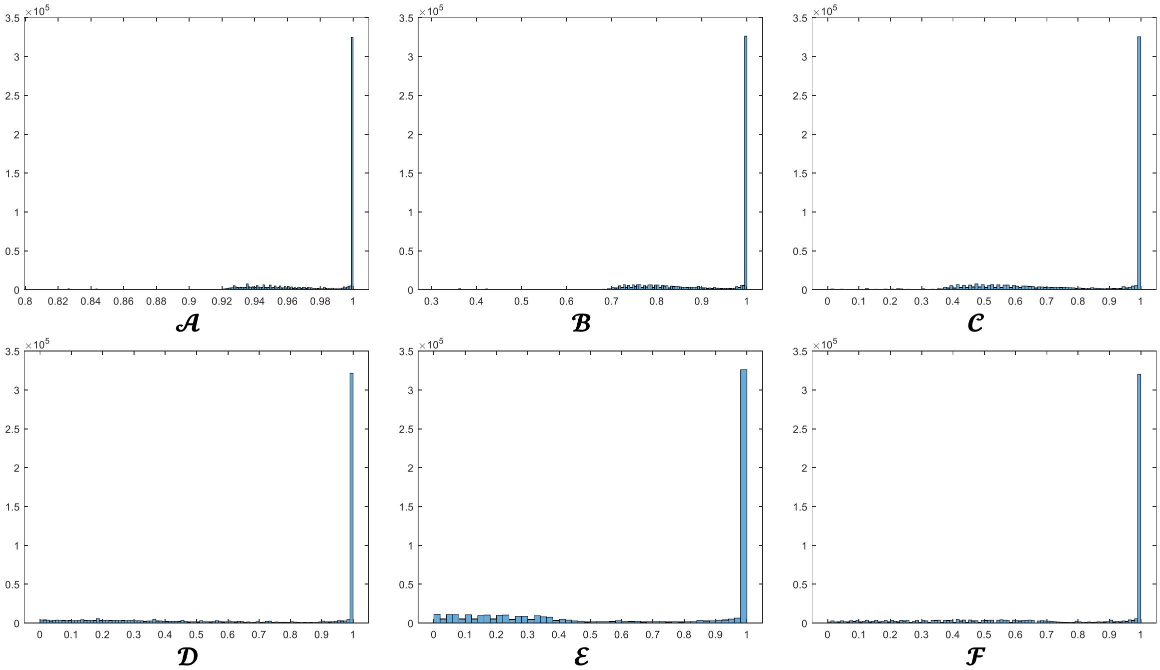

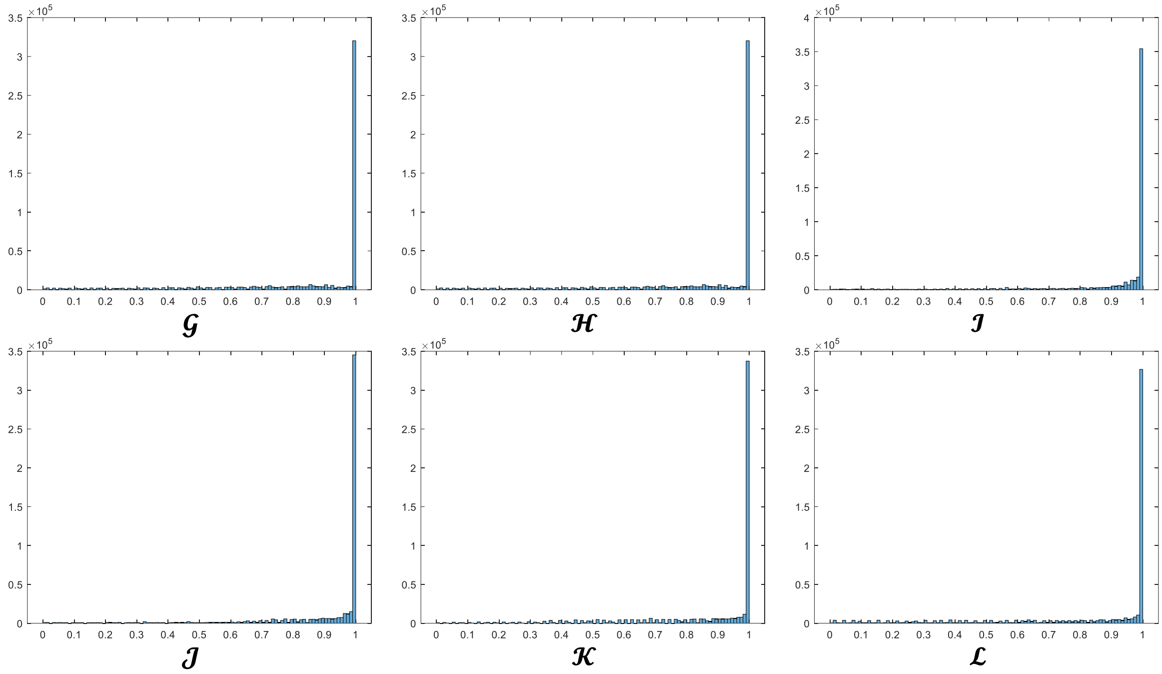

Figure 6. Histogram for MRI images ($\mathcal{A}$) Histogram for MRI image when $\mathcal{F}$ =0.1 ($\mathcal{B}$) Histogram for MRI image when $\mathcal{F}$ =0.2 ($\mathcal{C}$) Histogram for image MRI when $\mathcal{F}$ =0.3 ($\mathcal{D}$) Histogram for MRI image when $\mathcal{F}$ =0.4 ($\mathcal{E}$) Histogram for MRI image when $\mathcal{F}$ =0.5 ($\mathcal{F}$) Histogram for MRI image when $\mathcal{F}$ =0.6 ($\mathcal{G}$) Histogram for MRI image when $\mathcal{F}$ =0.7 ($\mathcal{H}$) Histogram for MRI image when $\mathcal{F}$ =0.8 ($\mathcal{I}$) Histogram for MRI image when $\mathcal{F}$ =0.9 ($\mathcal{J}$) Histogram for MRI image when $\mathcal{F}$ =1 ($\mathcal{K}$) Histogram for MRI image when $\mathcal{F}$ =1.1($\mathcal{L}$) Histogram for MRI image when $\mathcal{F}$ =1.2

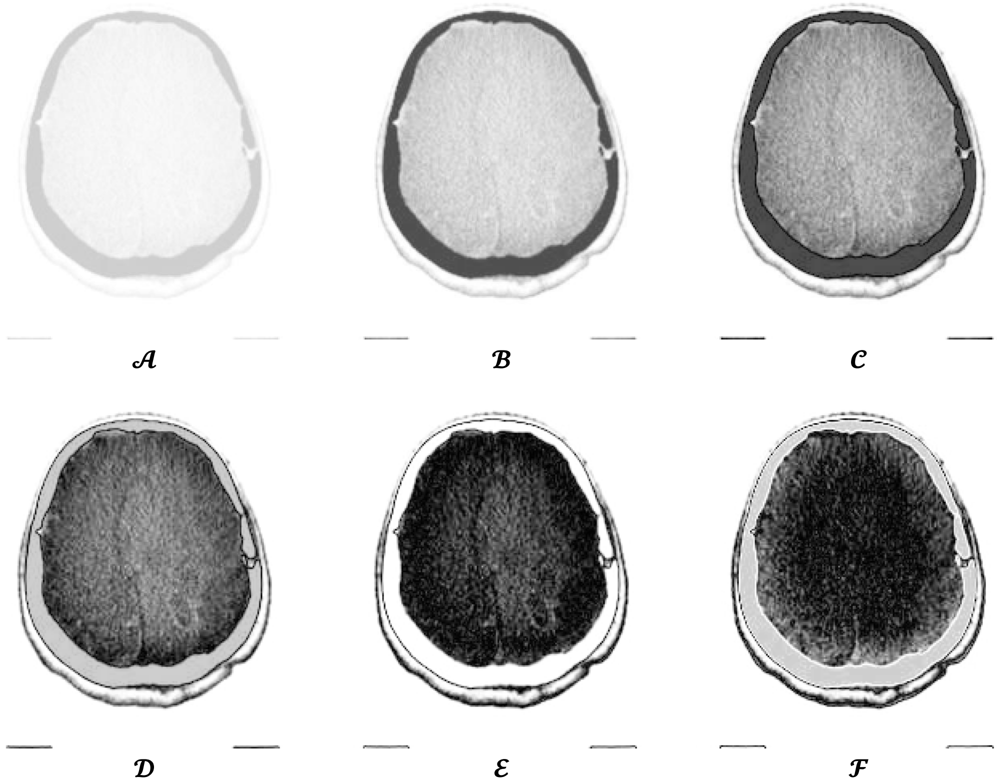

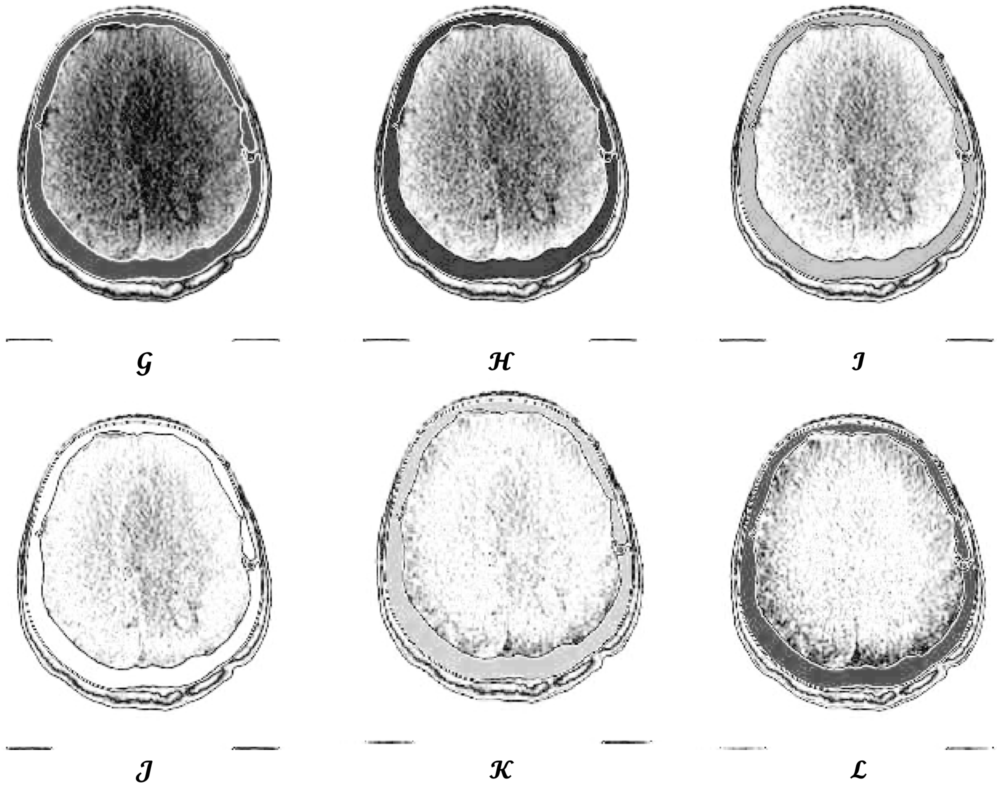

Figure 7. The resulting CT Scan images $\mathcal{A}$) resulting image when $\mathcal{F}$ =0.1 ($\mathcal{B}$) resulting image when $\mathcal{F}$ =0.2 ($\mathcal{C}$) resulting image when $\mathcal{F}$ =0.3 ($\mathcal{D}$) resulting image when $\mathcal{F}$ =0.4 ($\mathcal{E}$) resulting image when $\mathcal{F}$ =0.5 ($\mathcal{F}$) resulting image when $\mathcal{F}$ =0.6 ($\mathcal{G}$) resulting image when f=0.7 ($\mathcal{H}$) resulting image when $\mathcal{F}$ =0.8 ($\mathcal{I}$) resulting image when $\mathcal{F}$ =0.9 ($\mathcal{J}$) resulting image when $\mathcal{F}$ =1.1 ($\mathcal{K}$) resulting image when $\mathcal{F}$ =1.2($\mathcal{L}$) resulting image when f=0.9

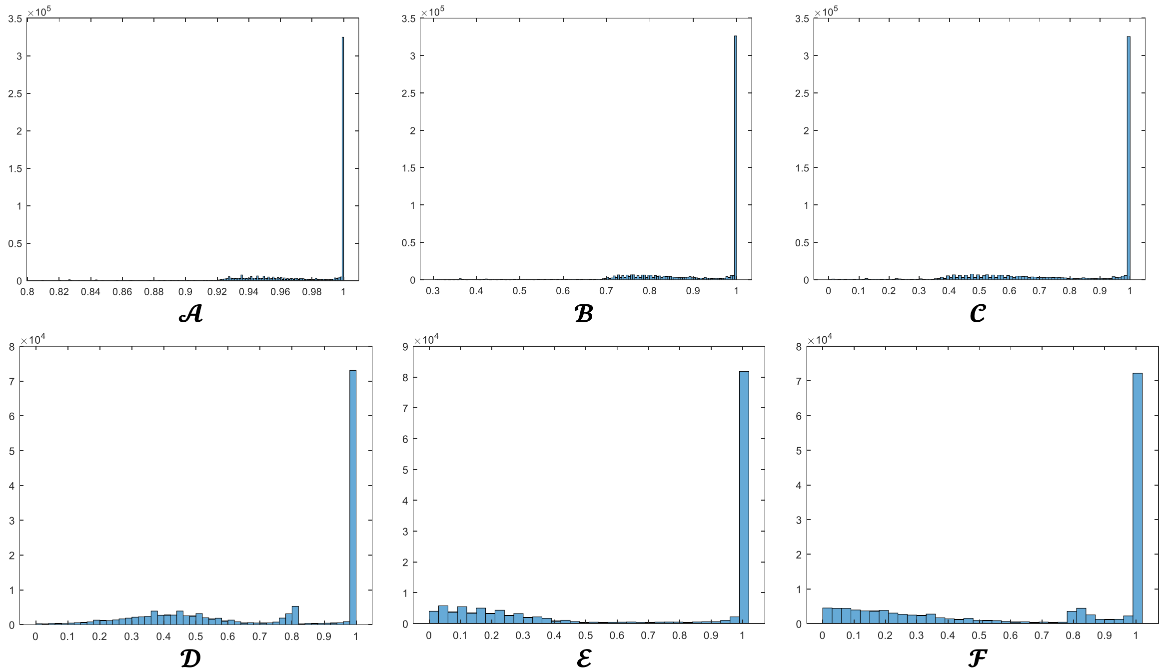

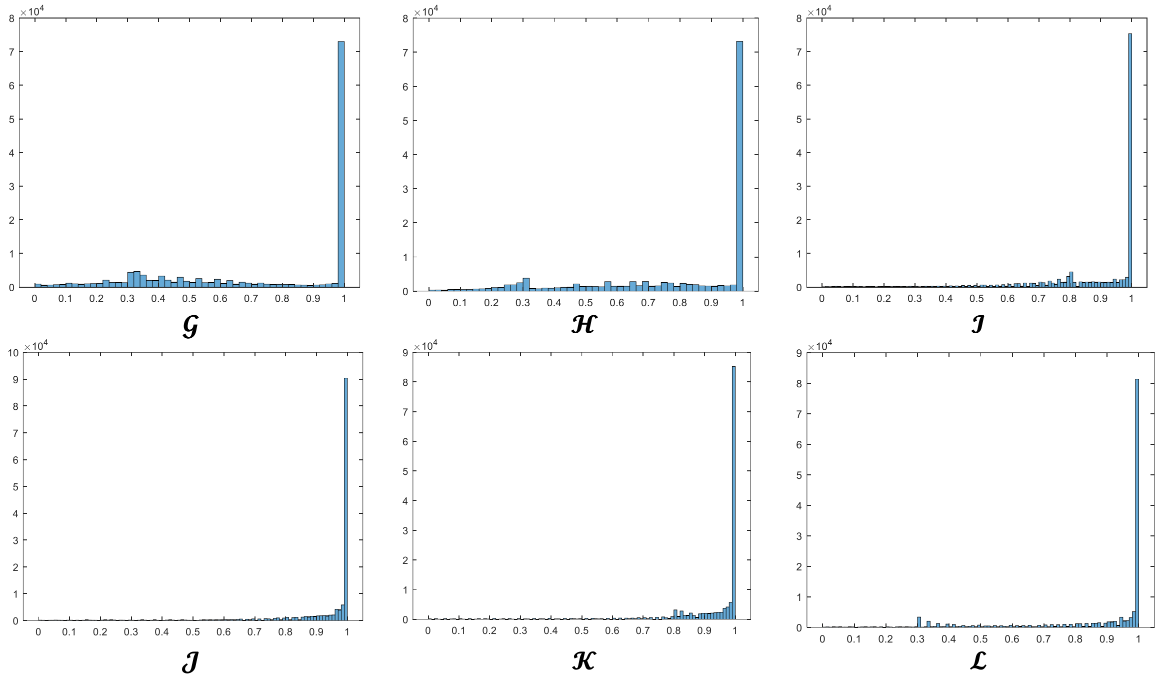

Figure 8. Histogram for CT Scan images ($\mathcal{A}$) Histogram for CT Scan image when $\mathcal{F}$ =0.1 ($\mathcal{B}$) Histogram for CT Scan image when $\mathcal{F}$ =0.2 ($\mathcal{C}$) Histogram for image CT Scan when $\mathcal{F}$ =0.3 ($\mathcal{D}$) Histogram for CT Scan image when $\mathcal{F}$ =0.4 ($\mathcal{E}$) Histogram for CT Scan image when $\mathcal{F}$ =0.5 ($\mathcal{F}$) Histogram for CT Scan image when $\mathcal{F}$ =0.6 ($\mathcal{G}$) Histogram for CT Scan image when $\mathcal{F}$ =0.7 ($\mathcal{H}$) Histogram for CT Scan image when $\mathcal{F}$ =0.8 ($\mathcal{I}$) Histogram for CT Scan image when $\mathcal{F}$ =0.9 ($\mathcal{J}$) Histogram for CT Scan image when $\mathcal{F}$ =1 ($\mathcal{K}$) Histogram for CT Scan image when $\mathcal{F}$ =1.1($\mathcal{L}$) Histogram for CT Scan image when $\mathcal{F}$ =1.2

8. Discussion

Experimental results showed that applying different F-factors directly impacted the quality of all types of medical images used in this study, including X-rays, MRIs, and CT scans.

1. As shown in **Figure 3** , which represents an enhanced X-ray image of a patient with nasal polyps using the proposed algorithm and varying F-factor values, the image is blurry, distorted, and lacks necessary detail, making diagnosis more difficult. When the F-factor values are equal to (0.4, 0.5, 0.6), the polyps begin to appear. At values of (0.7, 0.8, 0.9), the image becomes clear, and the polyps are easily visible. However, values of (1, 1.1, 1.2) result in excessive contrast enhancement, producing blurred images that can negatively impact diagnostic quality.

2. By observing **Figure 5** , which shows an enhanced MRI image of a patient with a brain tumour using the proposed algorithm and varying the F-values, the following was noted: when the F-values are equal to (0.1, 0.2), the resulting image is unclear, blurry, and lacks necessary detail, making diagnosis more difficult. As the F-values are equal to (0.3, 0.4, 0.5, 0.6), the tumour begins to appear. At F-values of (0.7, 0.8, or 0.9), the image becomes clear, and the tumour is easily visible. However, when the F-value is equal to (1, 1.1, 1.2), excessive contrast enhancement occurs, resulting in blurred images that can negatively impact diagnostic quality.

3. Similarly, **Figure 7.** presents an enhanced CT image of a patient with a brain tumour using the proposed algorithm and varying the F-values. At F-values of (0.1, 0.2), the image appears blurry, has high density, and lacks clear image details, making diagnosis more difficult. When the F-value is equal to (0.3, 0.4, 0.5, 0.6), the image is dominated by black, and the tumour is not visible. At F-values of (0.7, 0.8, and 0.9), the image becomes clear, and the tumour is easily identifiable. However, when the F-value is equal to (1, 1.1, 1.2), it results in excessive contrast enhancement, resulting in image noise, which can negatively impact diagnostic quality.

In general, F-values of (0, 0.8) have been identified as the most suitable for image enhancement in X-ray, MRI, and CT scans. It achieves the optimal balance between improving image quality and preserving original details, which contributes to increasing diagnostic accuracy and improving the interpretation of medical images. When observing the histogram in X-ray, MRI, and CT images before and after applying the enhancement algorithm, the original images displayed grey values between 0 and 1. Following the enhancement, the grey levels shifted toward higher values, or toward one, which shows how the algorithm affected the images. Contrast and lighting show that it was successful in enhancing the illumination in dim areas.

9. Conclusion

The main goal of image enhancement is to detect hidden features in images and increase the contrast in low-contrast images. These details play a crucial role in diagnosis, as some features are difficult to identify visually. Therefore, we often enhance images before displaying them. It is essential to focus on important features when displaying medical images. In this paper, an algorithm based on empirical equations is proposed, relying on trigonometric functions and varying the values of one of the main coefficients of the empirical equation F. Excellent results were obtained in diagnosing polyps in X-ray images, as well as in distinguishing brain tumours in MRI and CT scans. The best results were obtained when the F value was (0.8, 0.9). The algorithm's performance was evaluated through visual observation and histogram analysis before and after enhancement. The results showed improved contrast and detail resolution, demonstrating the efficiency of the proposed algorithm.

Conflict of Interest

On behalf of all authors, the corresponding author states that there is no conflict of interest.

Data Availability

No data was used for the research described in the article.

References

Agrawal, U. K., Panda, N., Mohanty, P., Mahapatra, M., Verma, S., & Singh, D. (2025). Advancements in Healthcare Medical Imaging through SHO optimized CNN. Procedia Computer Science, 258, 4128-4135.

Akbar, M. U., Wang, W., & Eklund, A. (2025). Beware of diffusion models for synthesizing medical images—a comparison with GANs in terms of memorizing brain MRI and chest x-ray images. Machine Learning: Science and Technology, 6(1), 015022.

Al-Khafaji, K. H., & Sahib, H. A. (2024). Designing a Digital System for Enhancing, Coloring, Encryption and Decryption of X-ray Medical Image. 2024 15th International Conference on Information and Communication Systems (ICICS),

Anitha, N., Rajesh, T., Parwekar, P., & Chatradi, N. R. (2024). Denoising and Quality Enhancement of CT Scan/X-Ray Images of Lung Disease for Enhanced Diagnosis. Proceedings of Eighth International Conference on Information System Design and Intelligent Applications,

Babu, B. S., & Venkatanarayana, D. M. (2024). MRI and CT image fusion using cartoon-texture and QWT decomposition and cuckoo search-grey wolf optimization. Multimedia Tools and Applications, 83(3), 8797-8835.

Chen, Z., Pawar, K., Ekanayake, M., Pain, C., Zhong, S., & Egan, G. F. (2023). Deep learning for image enhancement and correction in magnetic resonance imaging—state-of-the-art and challenges. Journal of Digital Imaging, 36(1), 204-230.

Dremel, K., Prjamkov, D., Firsching, M., Weule, M., Lang, T., Papadaki, A., Kasperl, S., Blaimer, M., & Fuchs, T. O. (2025). Utilizing Quantum Annealing in Computed Tomography Image Reconstruction. IEEE Transactions on Quantum

Engineering.

Falgout, D. M., Bevan, P. J., Grumet, R. C., & Parvaresh, K. C. (2024). Femoroacetabular impingement measurements obtained from two-dimensional radiographs versus three-dimensional–reconstructed computed tomography images result in different values. Arthroscopy, Sports Medicine, and Rehabilitation, 6(1), 100833.

Fan, J., Li, W., Zhou, Q., Yang, G., Tang, P., He, J., Ma, L., Zhang, J., Xiao, J., & Yan, Z. (2025). Metal Halide Perovskites for Direct X-Ray Detection in Medical Imaging: To Higher Performance. Advanced Functional Materials, 35(21), 2401017.

Gómez-Guzmán, M. A., Jiménez-Beristaín, L., García-Guerrero, E. E., López-Bonilla, O. R., Tamayo-Perez, U. J., Esqueda-Elizondo, J. J., Palomino-Vizcaino, K., & Inzunza-González, E. (2023). Classifying brain tumors on magnetic resonance imaging by using convolutional neural networks. Electronics, 12(4), 955.

Hussain, S., Mubeen, I., Ullah, N., Shah, S. S. U. D., Khan, B. A., Zahoor, M., Ullah, R., Khan, F. A., & Sultan, M. A. (2022). Modern diagnostic imaging technique applications and risk factors in the medical field: a review. BioMed research international, 2022(1), 5164970.

Idowu, O., Amusa, K., & Ilori, A. (2022). Improved enhancement technique for medical image processing. Am. J. Eng. Res. 2022 Am. J. Eng. Res.(AJER(11), 126-137.

Kumari, P. (2025). Transforming Medical Imaging With Convolutional Neural Networks (CNNs): Advances in Diagnosis and Treatment. Deep Learning in Medical Signal and Image Processing, 195-230.

Li, Y., Iwamoto, Y., & Chen, Y.-W. (2019). Medical Image Enhancement Using Deep Learning. In Deep Learning in Healthcare: Paradigms and Applications (pp. 53-76). Springer.

Mouzai, M., Mustapha, A., Bousmina, Z., Keskas, I., & Farhi, F. (2023). Xray-Net: Self-supervised pixel stretching approach to improve low-contrast medical imaging. Computers and Electrical Engineering, 110, 108859.

Nayak, K. S., Lim, Y., Campbell-Washburn, A. E., & Steeden, J. (2022). Real-time magnetic resonance imaging. Journal of Magnetic Resonance Imaging, 55(1), 81-99.

Ou, X., Chen, X., Xu, X., Xie, L., Chen, X., Hong, Z., Bai, H., Liu, X., Chen, Q., & Li, L. (2021). Recent development in x-ray imaging technology: Future and challenges. Research.

Pinto-Coelho, L. (2023). How artificial intelligence is shaping medical imaging technology: a survey of innovations and applications. Bioengineering, 10(12), 1435.

Pourasad, Y., & Cavallaro, F. (2021). A novel image processing approach to enhancement and compression of X-ray images. International Journal of Environmental Research and Public Health, 18(13), 6724.

Reda, R., Zanza, A., Mazzoni, A., Cicconetti, A., Testarelli, L., & Di Nardo, D. (2021). An update of the possible applications of magnetic resonance imaging (MRI) in dentistry: a literature review. Journal of imaging, 7(5), 75.

Rehman, A., & Mir, S. Q. (2025). Introduction to Medical Image Segmentation: Overview of Modalities, Benchmark Datasets, Data Augmentation Techniques, and Evaluation Metrics. Deep Learning Applications in Medical Image Segmentation: Overview, Approaches, and Challenges, 1-26.

Stewart, G. D., Godoy, A., Farquhar, F., Kitt, J., Cartledge, J., Kimuli, M., Rossi, S. H., Shinkins, B., Burbidge, S., & Burge, S. W. (2025). Abdominal noncontrast computed tomography scanning to screen for kidney cancer and other abdominal pathology within community-based computed tomography screening for lung cancer: results of the yorkshire kidney screening trial. European Urology, 87(5), 561-570.

Sule, D. S., & Ampofo, R. (2025). Diagnostic Imaging Techniques: Current Trends and Challenges. Diagnostic Advances in Precision Medicine and Drug Development, 49-66.

Yadav, P., & Donvir, A. (2025). Enhancing Medical Imaging Accessibility: An AI-Powered Automated Tactile and 3D-Printable X-Ray System. 2025 IEEE 15th Annual Computing and Communication Workshop and Conference (CCWC),